Initial value problem for magnetic fields in heavy ion collisions

Kirill Tuchin
Department of Physics and Astronomy, Iowa State University, Ames, Iowa 50011, USA
(Received 8 September 2015; published 19 January 2016)

When the quark-gluon plasma emerges in the wake of a heavy-ion collision, a magnetic field created by the valence charges has already permeated the entire interaction region. Evolution of this "initial" field in the plasma is governed by the Maxwell equations in an electrically conducting medium. As the plasma expands, external valence charges induce a magnetic field that also contributes to the total magnetic field in the plasma. I solve the initial value problem describing these processes and argue that the initial magnetic field often dominates over the one induced by the valence charges. In particular, it grows approximately proportional to the collision energy, unlike the induced component, which is energy independent. As a result, the magnetic field has a significant phenomenological influence on the quark-gluon plasma at CERN Large Hadron Collider energies over its entire lifetime.

DOI: 10.1103/PhysRevC.93.014905

I. INTRODUCTION

In this paper I reexamine the problem of the magnetic field created by electrical currents of colliding relativistic heavy ions [1–8]. Since these currents experience very little deflection in the course of collision [9,10] (and thus have large absolute values of rapidity), the corresponding magnetic field depends on the energy and geometry of the collision, and implicitly on the strong interaction dynamics through the electrical conductivity of the quark-gluon plasma (QGP) [2,6]. Another important aspect, which is the main focus of this study, is the transition dynamics from a magnetic field in vacuum to one in a medium.

To begin, assume that the QGP forms instantly at time $t = t_0$, where t is counted from the collision time in the laboratory frame. This time emerges in phenomenological models of QGP that favor rather small values compared to perturbation theory expectations; see, e.g., [11]. The earliest possible value of t_0 is determined by the saturation momentum Q_s as $1/Q_s$, and represents the time it takes to release most particles from the ion's wave functions. At the Relativistic Heavy Ion Collider (RHIC), $1/Q_s \sim 0.2$ fm. At $t < t_0$ we are dealing with the electromagnetic field created by the valence charges in vacuum. Its magnetic component is given by the well-known formula (7). At time $t = t_0$, when the QGP emerges, the magnetic field permeates the entire plasma. Starting at $t = t_0$ and thereafter, the behavior of the magnetic field is governed by the Maxwell equations in plasma. These equations describe evolution of the magnetic field in the electrically conducting QGP starting from its initial value at $t = t_0$. This component of the total magnetic field is referred to below as the "initial" magnetic field $\boldsymbol{B}_{\rm init}$. Another contribution to the magnetic field is induced by valence charges moving *outside* of the QGP, and is referred to below as the "valence" contribution $\boldsymbol{B}_{\rm val}$.[1] In previous publications the role of the initial field has not been properly recognized. In this paper I fill this void and, moreover, argue that in most cases the main contribution stems from the initial field.

The paper is organized as follows. In Secs. II–IV I deal with the magnetic field produced by a single point charge. In Sec. II I consider the magnetic field in vacuum, and in later sections in the electrically conducting QGP. The main result is given by Eqs. (34) and (35), which represent contributions of valence charges and the initial field respectively. A more realistic geometry is considered in Sec. V, where I discuss the case of two electric charges colliding at a given impact parameter b. I also discuss there the effect of time-dependent electrical conductivity on the magnetic field evolution. I discuss the results and summarize in Sec. VI.

II. MAGNETIC FIELD IN VACUUM

In a relativistic heavy-ion collision, an electromagnetic field is created by Z electric charges of one ion and Z electric charges of another ion moving in opposite directions along, say, the z axis such that the ion centers are at a distance b away. Due to the superposition principle, the total classical field is a sum of fields of all charges. Thus, in order to find the total field it is sufficient to solve for a single electric charge e. In this section I briefly review a textbook case of an electromagnetic field created in vacuum by a uniformly moving point charge e. Our intent here is to introduce notations, definitions etc.

Before the QGP formation, viz., at $t \leqslant t_0$, the vector potential $\boldsymbol{A}_1(\boldsymbol{r},t)$ of a point charge e moving along the trajectory $z = vt$ satisfies the equation

$$\nabla^2 \boldsymbol{A}_1(\boldsymbol{r},t) = \partial_t^2 \boldsymbol{A}_1(\boldsymbol{r},t) - \boldsymbol{j}(\boldsymbol{r},t), \tag{1}$$

where the electromagnetic current density due to a valence charge e is

$$\boldsymbol{j} = ev\hat{\boldsymbol{z}}\delta(z - vt)\delta(\boldsymbol{b}). \tag{2}$$

[1]To avoid confusion I emphasize that both components are ultimately related to electrical charges of heavy ions. The distinction only concerns our treatment of magnetic field at $t > t_0$, as will be explained in detail in the forthcoming sections.

 ©2016 American Physical Society

The momentum space representation is defined as

$$\boldsymbol{j}(\boldsymbol{r},t)=\int\frac{d^3k}{(2\pi)^3}e^{i\boldsymbol{k}\cdot\boldsymbol{r}}\boldsymbol{j}_{\boldsymbol{k}\omega}=\int\frac{d^2k_\perp dk_z}{(2\pi)^3}e^{i\boldsymbol{k}_\perp\cdot\boldsymbol{b}+ik_z z}\boldsymbol{j}_{\boldsymbol{k}\omega}. \tag{3}$$

With this normalization, the Fourier component of the current reads

$$\boldsymbol{j}_{\boldsymbol{k}}=ev\hat{\boldsymbol{z}}e^{-ik_z vt}. \tag{4}$$

It follows from (1) that the vector potential generated by the current (4) is

$$\boldsymbol{A}_{1\boldsymbol{k}}=\frac{2\pi ev\hat{\boldsymbol{z}}}{k^2-k_z^2v^2}=\frac{2\pi ev\hat{\boldsymbol{z}}}{k_z^2/\gamma^2+k_\perp^2}. \tag{5}$$

In the configuration space I obtain

$$\boldsymbol{A}_1(\boldsymbol{r},t)=\frac{\gamma ev\hat{\boldsymbol{z}}}{4\pi}\frac{1}{\sqrt{b^2+\gamma^2(vt-z)^2}}, \tag{6}$$

where $\gamma=(1-v^2)^{-1/2}$. The corresponding magnetic field

$$\boldsymbol{B}_1=-\partial_b A_1\hat{\boldsymbol{\phi}}=\frac{\gamma ev\hat{\boldsymbol{\phi}}}{4\pi}\frac{b}{(b^2+\gamma^2(vt-z)^2)^{3/2}}. \tag{7}$$

This solution is valid until $t=t_0$, at which time existence of an electrically conducting medium must be taken into account.

III. EXACT SOLUTION FOR CONSTANT ELECTRICAL CONDUCTIVITY

Maxwell's equations can be solved exactly for $t\geqslant t_0$ in the case of constant electrical conductivity σ. The vector potential $\boldsymbol{A}_2$ satisfies the equation

$$\nabla^2\boldsymbol{A}_2(\boldsymbol{r},t)=\partial_t^2\boldsymbol{A}_2(\boldsymbol{r},t)+\sigma\partial_t\boldsymbol{A}_2(\boldsymbol{r},t)-\boldsymbol{j}(\boldsymbol{r},t), \tag{8}$$

with the initial conditions

$$\boldsymbol{A}_2(\boldsymbol{r},t_0)=\boldsymbol{A}_1(\boldsymbol{r},t_0)\equiv\hat{\boldsymbol{z}}\Phi(\boldsymbol{r},t_0), \tag{9}$$

$$\partial_t\boldsymbol{A}_2(\boldsymbol{r},t_0)=\partial_t\boldsymbol{A}_1(\boldsymbol{r},t_0)\equiv\hat{\boldsymbol{z}}\Psi(\boldsymbol{r},t_0). \tag{10}$$

I stress that the current density $\boldsymbol{j}$ is due to electric charges outside the plasma. I assumed that permittivity and permeability of the QGP are trivial. One can take a more accurate account of the medium properties, which would yield more elaborate initial conditions. However, they are not expected to significantly change the final result.

In momentum space Eq. (8) and the corresponding initial conditions (9) and (10) read

$$-k^2\boldsymbol{A}_{2\boldsymbol{k}}(t)=\partial_t^2\boldsymbol{A}_{2\boldsymbol{k}}(t)+\sigma\partial_t\boldsymbol{A}_{2\boldsymbol{k}}(t)-ev\hat{\boldsymbol{z}}e^{-ik_z vt}, \tag{11}$$

$$\boldsymbol{A}_{2\boldsymbol{k}}(t_0)=\hat{\boldsymbol{z}}\Phi_{\boldsymbol{k}}(t_0)=\frac{ev\hat{\boldsymbol{z}}}{k_z^2/\gamma^2+k_\perp^2}e^{-ik_z vt_0}, \tag{12}$$

$$\partial_t\boldsymbol{A}_{2\boldsymbol{k}}(t_0)=\hat{\boldsymbol{z}}\Psi_{\boldsymbol{k}}(t_0)=-ik_z v\frac{ev\hat{\boldsymbol{z}}}{k_z^2/\gamma^2+k_\perp^2}e^{-ik_z vt_0}. \tag{13}$$

To solve (11), I first consider the corresponding homogeneous equation

$$-k^2a_{\boldsymbol{k}}(t)=\partial_t^2a_{\boldsymbol{k}}(t)+\sigma\partial_t a_{\boldsymbol{k}}(t), \tag{14}$$

Seeking its solution in the form $a_{\boldsymbol{k}}\propto e^{-i\omega t}$ I find, upon substitution into (14), that ω must obey one of the dispersion relations

$$\omega=\omega_\pm=-\frac{i\sigma}{2}\pm\sqrt{k^2-\frac{\sigma^2}{4}}. \tag{15}$$

Thus, the general solution of the homogeneous equation (14), which describes propagation of the initial conditions, reads

$$a_{\boldsymbol{k}}(t)=\alpha e^{-i\omega_+(t-t_0)}+\beta e^{-i\omega_-(t-t_0)}, \tag{16}$$

where α and β are constants to be determined from the initial conditions (12) and (13). The particular solution due to the external current density is of the form $A_{2\boldsymbol{k}}\propto\delta e^{-ik_z vt}$, where δ is found upon substitution into (11):

$$\delta=\frac{ev}{k^2-k_z^2v^2-ik_z v\sigma}. \tag{17}$$

Thus, the general solution to (11) is

$$\boldsymbol{A}_{2\boldsymbol{k}}=\hat{\boldsymbol{z}}\Big\{\alpha e^{-i\omega_+(t-t_0)}+\beta e^{-i\omega_-(t-t_0)}+\frac{ev}{k^2-k_z^2v^2-ik_z v\sigma}e^{-ik_z vt}\Big\}. \tag{18}$$

Applying the initial conditions (12) and (13), I can fix α and β. The final result is

$$\begin{aligned}\boldsymbol{A}_{2\boldsymbol{k}}=\hat{\boldsymbol{z}}\Big\{&\delta\Big[\Big(\frac{\omega_--k_z v}{\omega_+-\omega_-}e^{-i\omega_+(t-t_0)}-\frac{\omega_+-k_z v}{\omega_+-\omega_-}e^{-i\omega_-(t-t_0)}\Big)\\&\times e^{-ik_z vt_0}+e^{-ik_z vt}\Big]\\&+\frac{1}{i(\omega_+-\omega_-)}\Phi_{\boldsymbol{k}}[-i\omega_-e^{-i\omega_+(t-t_0)}+i\omega_+e^{-i\omega_-(t-t_0)}]\\&+\frac{1}{i(\omega_+-\omega_-)}\Psi_{\boldsymbol{k}}[-e^{-i\omega_+(t-t_0)}+e^{-i\omega_-(t-t_0)}]\Big\}.\end{aligned} \tag{19}$$

Fourier transformation to the configuration space yields exact an analytical solution to the initial-value problem (8)–(10). Analytical and numerical evaluations of the integral over $\boldsymbol{k}$ are challenging. Fortunately, in the ultrarelativistic limit $\gamma\gg1$, which is relevant for relativistic heavy-ion collisions, the expression for the vector potential (19) is significantly simplified [6]. This is the subject of the next section.

IV. DIFFUSION APPROXIMATION

For an ultrarelativistic charge moving along the trajectory $z=vt$, $\partial_t^2-\partial_z^2\sim k_z^2/\gamma^2\ll k_\perp^2,\sigma k_z$, which implies $\sigma\gamma\gg k_\perp$ [6]. In this case (8) can be approximated by

$$\nabla_\perp^2\boldsymbol{A}_2(\boldsymbol{r},t)=\sigma\partial_t\boldsymbol{A}_2(\boldsymbol{r},t)-\boldsymbol{j}(\boldsymbol{r},t). \tag{20}$$

This approximation holds even in the case of time-dependent conductivity, provided that such dependence is adiabatic, which is a reasonable approximation for a realistic plasma. Since (20) is of the first order in the time derivative, it requires only one initial condition,

$$\boldsymbol{A}_2(\boldsymbol{r},t_0)=\boldsymbol{A}_1(\boldsymbol{r},t_0)=\hat{\boldsymbol{z}}\Phi(\boldsymbol{r},t_0). \tag{21}$$

I can solve the initial-value problem (20)–(21) for an arbitrary time dependence of the conductivity $\sigma(t)$. Introducing a new "time" variable λ according to

$$\lambda(t) = \int_{t_0}^{t} \frac{dt'}{\sigma(t')} \tag{22}$$

and transferring (20) to the momentum space, I obtain

$$-k_\perp^2 \boldsymbol{A}_{2\boldsymbol{k}} = \partial_\lambda \boldsymbol{A}_{2\boldsymbol{k}} - \boldsymbol{j}_{\boldsymbol{k}}\,. \tag{23}$$

The corresponding homogeneous equation [i.e., (23) with $\boldsymbol{j}_{\boldsymbol{k}} = 0$] is solved by

$$\boldsymbol{a}_{\boldsymbol{k}}(\lambda) = \hat{\boldsymbol{z}} C e^{-k_\perp^2 \lambda}, \tag{24}$$

where C is a constant. To derive a particular solution, I treat C as a function of λ and plug into (23). I get

$$C = ev \int_0^{\lambda} d\lambda' e^{k_\perp^2 \lambda' - ik_z v t(\lambda')} + D. \tag{25}$$

Substituting into (24) I find the general solution to (23),

$$\boldsymbol{A}_{2\boldsymbol{k}}(t) = \hat{\boldsymbol{z}}\left\{ev e^{-k_\perp^2\lambda} \int_0^{\lambda} d\lambda' e^{k_\perp^2\lambda' - ik_z v t(\lambda')} + De^{-k_\perp^2\lambda}\right\}. \tag{26}$$

Since $\lambda(t_0) = 0$, the initial condition (21) implies that $D = \Phi_{\boldsymbol{k}}(\boldsymbol{r}, t_0)$. So finally,

$$\boldsymbol{A}_{2\boldsymbol{k}}(t) = \hat{\boldsymbol{z}}\left\{ev e^{-k_\perp^2\lambda(t)} \int_{t_0}^{t} \frac{dt'}{\sigma(t')} e^{k_\perp^2\lambda(t') - ik_z v t'} + \Phi_{\boldsymbol{k}} e^{-k_\perp^2\lambda(t')}\right\}. \tag{27}$$

In the particular case of constant electrical conductivity, (27) simplifies to

$$\boldsymbol{A}_{2\boldsymbol{k}}(t) = \hat{\boldsymbol{z}}\left\{\frac{ev}{\sigma}\frac{1}{\frac{k_\perp^2}{\sigma} - ik_z v}\left(e^{-ik_z v t} - e^{-\frac{k_\perp^2}{\sigma}(t-t_0)} e^{-ik_z v t_0}\right) + \Phi_{\boldsymbol{k}} e^{-\frac{k_\perp^2}{\sigma}(t-t_0)}\right\}. \tag{28}$$

This expression can be derived directly from (19), but the approach described in this section is more straightforward. Fourier transformation to the configuration space,

$$\boldsymbol{A}_2(\boldsymbol{r}, t) = \int \frac{d^2k_\perp}{(2\pi)^2} \int_{-\infty}^{+\infty} \frac{dk_z}{2\pi} e^{i\boldsymbol{k}_\perp\cdot\boldsymbol{b} + ik_z z} \boldsymbol{A}_{2\boldsymbol{k}}(t), \tag{29}$$

can be done using the following integrals:

$$\int \frac{d^2k_\perp}{(2\pi)^2} \int_{-\infty}^{+\infty} \frac{dk_z}{2\pi} e^{i\boldsymbol{k}_\perp\cdot\boldsymbol{b} + ik_z z} e^{-k_\perp^2[\lambda(t) - \lambda(t')]} = \frac{\exp\left\{-\frac{b^2}{4[\lambda(t)-\lambda(t')]}\right\}}{4[\lambda(t) - \lambda(t')]}\delta(z - vt'), \tag{30}$$

$$\int \frac{d^2k_\perp}{(2\pi)^2} \int_{-\infty}^{+\infty} \frac{dk_z}{2\pi} e^{i\boldsymbol{k}_\perp\cdot\boldsymbol{b} + ik_z z} e^{-k_\perp^2\lambda(t)} \frac{ev}{k_z^2/\gamma^2 + k_\perp^2} e^{-ik_z v t_0} = \frac{\gamma ev}{4\pi}\int_0^{\infty} dk_\perp J_0(k_\perp b) e^{-k_\perp^2\lambda(t) - k_\perp\gamma|z - vt_0|}. \tag{31}$$

Substituting (27) into (29), doing integrals (30) and (31), and then integrating over t' yields

$$\boldsymbol{A}_2(\boldsymbol{r}, t) = \frac{\hat{\boldsymbol{z}} e}{4\sigma(z/v)} \frac{\exp\left\{-\frac{b^2}{4[\lambda(t)-\lambda(z/v)]}\right\}}{4[\lambda(t) - \lambda(z/v)]}\theta(tv - z)\theta(z - vt_0) + \frac{\gamma ev\hat{\boldsymbol{z}}}{4\pi}\int_0^{\infty} dk_\perp J_0(k_\perp b) e^{-k_\perp^2\lambda(t) - k_\perp\gamma|z - vt_0|}. \tag{32}$$

The magnetic field can be calculated as in (7) with the result

$$\boldsymbol{B}_2 = \boldsymbol{B}_{\rm val} + \boldsymbol{B}_{\rm init}\,, \tag{33}$$

where the "valence" $\boldsymbol{B}_{\rm val}$ and "initial" $\boldsymbol{B}_{\rm init}$ components are given by

$$e\boldsymbol{B}_{\rm val}(\boldsymbol{r}, t) = \hat{\boldsymbol{\phi}}\frac{\alpha\pi b}{2\sigma(z/v)[\lambda(t) - \lambda(z/v)]^2} \times \exp\left\{-\frac{b^2}{4[\lambda(t) - \lambda(z/v)]}\right\} \times\theta(tv - z)\theta(z - vt_0), \tag{34}$$

$$e\boldsymbol{B}_{\rm init}(\boldsymbol{r}, t) = \hat{\boldsymbol{\phi}}\gamma\alpha v \int_0^{\infty} dk_\perp k_\perp J_1(k_\perp b) \times \exp\{-k_\perp^2\lambda(t) - k_\perp\gamma|z - vt_0|\}. \tag{35}$$

The fine structure constant $\alpha = e^2/(4\pi)$. Note that at $t = t_0$, $\boldsymbol{B}_{\rm val}$ vanishes whereas $\boldsymbol{B}_{\rm init}$ yields the initial condition (7). $\boldsymbol{B}_{\rm init}$ is the field that permeates the plasma as it emerges at $t = t_0$ (at which time it coincides with $\boldsymbol{B}_1$) and spreads in it according to (35). Unlike $\boldsymbol{B}_{\rm val}$, it strongly depends on the collision energy 2γ (in units of proton mass).

$\boldsymbol{B}_{\rm val}$ describes the induced electromagnetic field generated as a response of the QGP to the electromagnetic field of the valence charge, and builds up starting from $t = t_0$. Because of the two step-functions in (34) that reflect causality, $\boldsymbol{B}_{\rm val}$ is finite only in the interval $vt_0 \leqslant z \leqslant vt$. In particular, it vanishes at midrapidity, $z = 0$. At fixed z satisfying $z \geqslant vt_0$, $\boldsymbol{B}_{\rm val}$ emerges when $t = z/v$. An important property of $\boldsymbol{B}_{\rm val}$ is that its magnitude is independent of energy (since $v \approx 1$).

At early times after the QGP creation, viz., $t \gtrsim t_0$, the expression in the exponent of (35) is such that $k_\perp^2\lambda \ll k_\perp\gamma|z - vt_0|$, implying that $\boldsymbol{B}_{\rm init} \approx \boldsymbol{B}_1$. However, at later times when $k_\perp^2\lambda \gg k_\perp\gamma|z - vt_0|$, I get

$$e\boldsymbol{B}_{\rm init} = \hat{\boldsymbol{\phi}}\frac{\gamma\alpha v b\sqrt{\pi}}{8\lambda^{3/2}} e^{-\frac{b^2}{8\lambda}}\left[I_0\left(\frac{b^2}{8\lambda}\right) - I_1\left(\frac{b^2}{8\lambda}\right)\right]. \tag{36}$$

Since $k_\perp b \sim \sqrt{8}$ (which can be seen from J_1 series expansion) and $\lambda \sim (t - t_0)/\sigma$, I estimate that (36) is valid at times t satisfying

$$\frac{t - t_0}{|z - vt_0|} \gg \frac{1}{\sqrt{8}}\gamma\sigma b. \tag{37}$$

At $z = 0$, $b = 7$ fm, and $t_0 = 0.2$ fm this implies $t \gg 1$ fm, where I used $\sigma = 5.8$ MeV known from the lattice calculations [12]; see also [13–15]. Furthermore, since $b^2/8\lambda \ll 1$, I expand (36) to obtain the late-time behavior of the initial

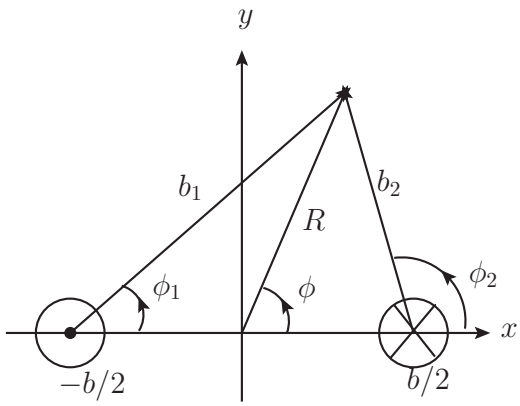

FIG. 1. Two counterpropagating charges e. One charge moves along the positive z axis at $z = vt$, $x = -b/2$, $y = 0$ while another one moves in the opposite direction at $z = -vt$, $x = b/2$, $y = 0$.

magnetic field,

$$e\boldsymbol{B}_{\rm init} \approx \frac{\gamma\alpha v\sqrt{\pi}b}{8\lambda^{3/2}}\hat{\boldsymbol{\phi}}. \tag{38}$$

For constant σ the late-time dependence (viz., $t \gg t_0$) is $B_{\rm init} \sim 1/t^{3/2}$. Notice that at late times the "valence" contribution decays as $B_{\rm val} \sim 1/t^2$. It therefore emerges that the initial magnetic field dominates at early and late times.

V. MAGNETIC FIELD OF TWO COUNTERPROPAGATING CHARGES

To calculate the magnetic field in a heavy-ion collision, one considers two sets of Z counterpropagating electric charges distributed according to one of the known nuclear density parametrizations; see, e.g., [3]. However, to study the time evolution of the magnetic field it suffices to consider just two counterpropagating charges. The geometric symmetry of this configuration is similar to that of the event average over many heavy-ion collisions at impact parameter b, but drastically reduces the computational time. The configuration that I consider is depicted in Fig. 1.

Let $B^{(1)}(\boldsymbol{r}_1,t)$ and $B^{(2)}(\boldsymbol{r}_2,t)$ be magnitudes of the fields of the two charges, each given by (33)–(35). I can express coordinates of the observation point relative to each charge $\boldsymbol{r}_1 = \boldsymbol{b}_1 + \hat{z}z_1$ and $\boldsymbol{r}_2 = \boldsymbol{b}_2 + \hat{z}z_2$ in terms of their centers of mass in cylindrical coordinates R,z,ϕ as follows (see Fig. 1):

$$b_a = \sqrt{b^2/4 + R^2 + (-1)^a\, bR\cos\phi}\,,$$
$$\tan\phi_a = \frac{R\sin\phi}{R\cos\phi - (-1)^a\, b/2}, \quad z_a = vt + (-1)^a z. \tag{39}$$

where $a = 1,2$ labels the charges. Noting that $\boldsymbol{B}^{(a)} \propto \hat{\boldsymbol{\phi}}_a$ and expressing $\hat{\boldsymbol{\phi}}_a$ in terms of $\hat{\boldsymbol{b}}$ and $\hat{\boldsymbol{\phi}}$, I obtain the magnetic field in terms of the center-of-mass frame coordinates:

$$\boldsymbol{B} = \hat{\boldsymbol{b}}[B^{(1)}(\boldsymbol{r}_1,t)\sin(\phi-\phi_1) + B^{(2)}(\boldsymbol{r}_2,t)\sin(\phi-\phi_2)] + \hat{\boldsymbol{\phi}}[B^{(1)}(\boldsymbol{r}_1,t)\cos(\phi-\phi_1) + B^{(2)}(\boldsymbol{r}_2,t)\cos(\phi-\phi_2)], \tag{40}$$

where $\boldsymbol{r}_a$ and ϕ_a are replaced as indicated in (39). The result is shown in Figs. 2–5 in terms of a dimensionless and unit-independent quantity eB/m_π^2. In all figures the impact parameter is $b = 1$ fm, the observation point is at $\phi = \pi/2$, $R = 7$ fm (i.e,. $x = 0$ and $y = 7$ fm), and $\gamma = 100$ (except Fig. 4). Also indicated is the pseudorapidity $\eta = -\ln[-(z/R) + \sqrt{(z/R)^2 + 1}\,]$. Solid lines indicate the total magnetic field B, dashed lines represent the contribution of the initial condition $B_{\rm init}$, and dotted lines stand for the contribution of the valence charges $B_{\rm val}$. As discussed at the end of the previous section, the valence charge contribution decreases with time faster than that of the initial condition.

Figures 2–4 depict the magnetic field at constant electrical conductivity $\sigma = 5.8$ MeV [12]. In Fig. 2 I compare the magnetic field that is generated when the QGP emerges at $t_0 = 0.2$ fm with that at $t_0 = 0.5$ fm. Since the magnetic field in vacuum decreases as $1/t^3$, see (7), the late emergence of the conducting medium means that the magnitude of the field in the former case is about 15 times larger than in the latter. In both cases time dependence of magnetic field in the plasma is mild. Because of the step functions in (34), the magnetic field at midrapidity, $z = 0$, is entirely due to the initial field $B_{\rm init}$.

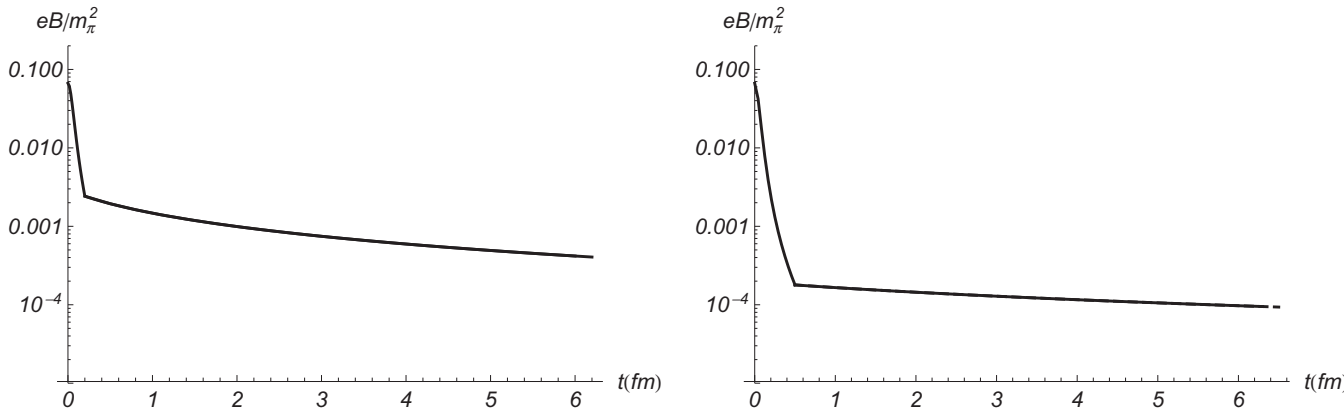

FIG. 2. Magnetic field in units of m_π^2/e. $\sigma = 5.8$ MeV, $z = 0$ fm ($\eta = 0$). Left panel: $t_0 = 0.2$ fm; right panel: $t_0 = 0.5$ fm. The valence current does not contribute at all ($B_{\rm val} = 0$).

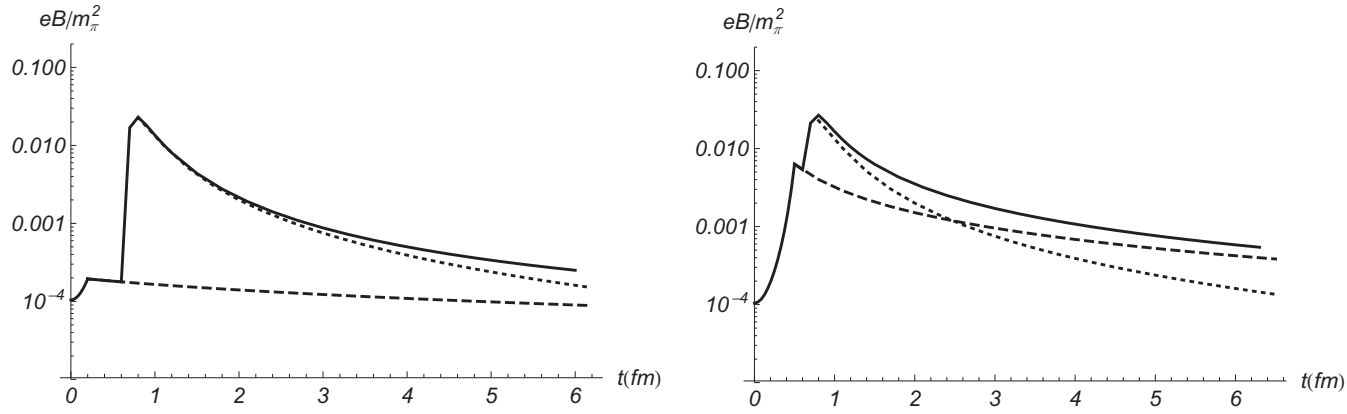

FIG. 3. Magnetic field in units of m_π^2/e. $\sigma = 5.8$ MeV, $z = 0.6$ fm ($\eta = 0.086$). Left panel: $t_0 = 0.2$ fm; right panel: $t_0 = 0.5$ fm. Solid, dashed, and dotted lines stand for B, $B_{\rm init}$, and $B_{\rm val}$.

Figure 3 is similar to Fig. 2 except that $z = 0.6$ fm, unlocking the "valence" contribution. Being independent of the initial value of the magnetic field at t_0, the valence contribution rapidly increases to its maximal value, which can be determined from (34) [16]. It then decreases at larger t and becomes smaller than $B_{\rm init}$. Sharp lines seen in Fig. 3 indicate that the transition dynamics near $t = t_0$ is not fully captured by the diffusion approximation.

The energy dependence of the magnetic field between RHIC and Large Hadron Collider (LHC) energies can be seen in Fig. 4. $B_{\rm init}$ grows approximately proportional to the collision energy γ, whereas $B_{\rm val}$ is energy independent. Thus, at the LHC the magnetic field induced by valence charges is negligible.

So far I considered only the case of constant electrical conductivity. In practice, however electrical conductivity is time dependent. To see the impact of σ time dependence on the time evolution of magnetic field I consider two models. In model A I assume that the QGP emerges instantly at $t = t_0$ with $\sigma = 5.8$ MeV and then cools down as it expands according to the Bjorken scenario [17]. Namely, expansion is supposed to be isentropic, $nV = \text{const}$, where n is the particle number density and V is plasma volume. Since $n \sim T^3$ and at early times expansion is one-dimensional, $V \sim t$, it follows that $T \propto t^{-1/3}$. Since $\sigma(t) \propto T$, I conclude that $\sigma(t) \sim t^{-1/3}$. Thus a reasonable model for time dependence of electrical conductivity is

$$\sigma(t) = \frac{\sigma}{2^{-1/3}(1 + t/t_0)^{1/3}}, \quad \text{model A.} \tag{41}$$

Another possibility is that the QGP does not appear as a thermal medium right away at $t = t_0$, rather it takes time τ until the conductivity reaches its equilibrium value σ. This can be described as

$$\sigma(t) = \sigma(1 - e^{-t/\tau}), \quad \text{model B.} \tag{42}$$

I set conservatively $\tau = 1$ fm. Note that I cannot let $\sigma(t)$ vanish at $t = t_0$ because that would violate the diffusion approximation that leads to (20). However, (42) insures that $\sigma(t_0) \ll \sigma$.

In Fig. 5 I contrast the two models. A similar calculation at constant conductivity is shown in the left panel of Fig. 4. I observe that time dependence (41) (model A) significantly reduces the magnetic field at later times. As far as model B is concerned, time dependence (42) affects mostly $B_{\rm val}$ because it directly depends on $\sigma(t)$, whereas $B_{\rm init}$ depends only on

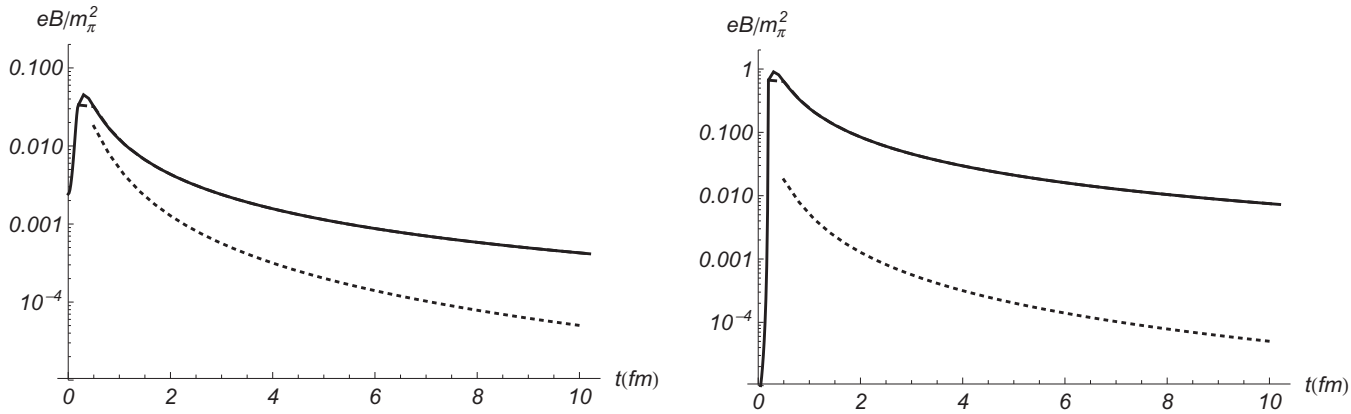

FIG. 4. Magnetic field in units of m_π^2/e. $\sigma = 5.8$ MeV, $z = 0.2$ fm, $t_0 = 0.2$ fm. Solid, dashed, and dotted lines stand for B, $B_{\rm init}$, and $B_{\rm val}$. Left panel: $\gamma = 100$ (RHIC); right panel: $\gamma = 2000$ (LHC).

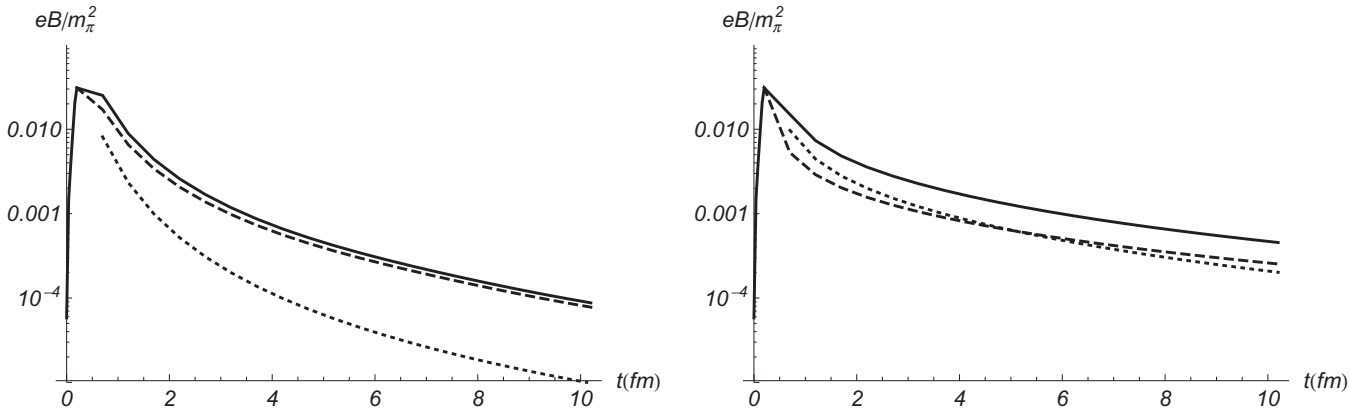

FIG. 5. Magnetic field in units of m_π^2/e. $z = 0.2$ fm, $t_0 = 0.2$ fm. Left panel: model A. Right panel: model B. Solid, dashed, and dotted lines stand for B, $B_{\rm init}$, and $B_{\rm val}$.

$\lambda(t)$; see (34) and (35). Model B has minor effect on the total magnetic field, although one can certainly find regions in space-time where its effect is more pronounced. What actually matters is the initial time t_0 at which one can treat the produced particle system as a medium. As long as conductivity is large enough at later times, the magnetic field is fairly insensitive to the precise QGP dynamics.

VI. SUMMARY

Just before the QGP emerges, the interaction region is permeated by the primordial electromagnetic field created by valence charges of two heavy ions. At the initial time t_0, this magnetic field smoothly connects to the magnetic field in the plasma and evolves according to the Maxwell equations in the electrically conducting medium. In addition to this "initial" magnetic field, there is another "valence" contribution that arises from the external valence electric charges inducing currents in the QGP. It has been tacitly assumed that the former contribution is not important [6]. In this paper I argued, to the contrary, that the initial magnetic field dominates at very early and later times and increases much faster with the collision energy than the "valence" contribution.

I also studied the effect of time dependence of electrical conductivity and concluded that at early times it has a rather minor effect on the field strength, as long as the produced particle system can be treated as a medium at early enough time. However, towards the later times of plasma evolution, time dependence of electrical conductivity plays an important role. In the Bjorken scenario it leads to much weaker fields compared to the constant conductivity case.

I considered the case of two counterpropagating charges, which gives an accurate picture of the time dependence of the event-averaged fields in heavy-ion collisions. Scaling the result with Z, I can obtain an estimate of the magnetic field strength in heavy-ion collisions. Calculating the spatial distribution requires an accurate account of the exact nuclear geometry, which is not difficult using the results reported in this paper.

ACKNOWLEDGMENTS

This work was supported in part by the U.S. Department of Energy under Grant No. DE-FG02-87ER40371.

[1] V. Skokov, A. Y. Illarionov, and V. Toneev, Estimate of the magnetic field strength in heavy-ion collisions, Int. J. Mod. Phys. A **24**, 5925 (2009).
[2] K. Tuchin, Synchrotron radiation by fast fermions in heavy-ion collisions, Phys. Rev. C **82**, 034904 (2010); Erratum: Synchrotron radiation by fast fermions in heavy-ion collisions, **83**, 039903(E) (2011).
[3] A. Bzdak and V. Skokov, Event-by-event fluctuations of magnetic and electric fields in heavy ion collisions, Phys. Lett. B **710**, 171 (2012).
[4] V. Voronyuk, V. D. Toneev, W. Cassing, E. L. Bratkovskaya, V. P. Konchakovski, and S. A. Voloshin, (Electro-)Magnetic field evolution in relativistic heavy-ion collisions, Phys. Rev. C **83**, 054911 (2011).
[5] W.-T. Deng and X.-G. Huang, Event-by-event generation of electromagnetic fields in heavy-ion collisions, Phys. Rev. C **85**, 044907 (2012).
[6] K. Tuchin, Time and space dependence of the electromagnetic field in relativistic heavy-ion collisions, Phys. Rev. C **88**, 024911 (2013).
[7] L. McLerran and V. Skokov, Comments about the electromagnetic field in heavy-ion collisions, Nucl. Phys. A **929**, 184 (2014).
[8] B. G. Zakharov, Electromagnetic response of quark-gluon plasma in heavy-ion collisions, Phys. Lett. B **737**, 262 (2014).
[9] K. Itakura, Y. V. Kovchegov, L. McLerran, and D. Teaney, Baryon stopping and valence quark distribution at small x, Nucl. Phys. A **730**, 160 (2004).
[10] D. Kharzeev, Can gluons trace baryon number?, Phys. Lett. B **378**, 238 (1996).
[11] P. F. Kolb and U. W. Heinz, Hydrodynamic description of ultrarelativistic heavy ion collisions, in *Quark Gluon Plasma*, edited by R. C. Hwa (World Scientific, Singapore, 1990), pp. 634–714.

[12] H.-T. Ding, A. Francis, O. Kaczmarek, F. Karsch, E. Laermann, and W. Soeldner, Thermal dilepton rate and electrical conductivity: An analysis of vector current correlation functions in quenched lattice QCD, Phys. Rev. D **83**, 034504 (2011).

[13] G. Aarts, C. Allton, J. Foley, S. Hands, and S. Kim, Spectral functions at small energies and the electrical conductivity in hot, quenched lattice QCD, Phys. Rev. Lett. **99**, 022002 (2007).

[14] G. Aarts, C. Allton, A. Amato, P. Giudice, S. Hands, and J. I. Skullerud, Electrical conductivity and charge diffusion in thermal QCD from the lattice, J. High Energy Phys. 02 (2015) 186.

[15] W. Cassing, O. Linnyk, T. Steinert and V. Ozvenchuk, On the electric conductivity of hot QCD matter, Phys. Rev. Lett. **110**, 182301 (2013).

[16] K. Tuchin, Particle production in strong electromagnetic fields in relativistic heavy-ion collisions, Adv. High Energy Phys. **2013**, 1 (2013).

[17] J. D. Bjorken, Highly relativistic nucleus-nucleus collisions: The central rapidity region, Phys. Rev. D **27**, 140 (1983).